Supplementary Online Content

Sudre G, Choudhuri S, Szekely E, et al. Estimating the heritability of structural and functional brain connectivity in families affected by attention-deficit/hyperactivity disorder. *JAMA Psychiatry*. Published online November 16, 2016. doi:10.1001/jamapsychiatry.2016.3072

This supplementary material has been provided by the authors to give readers additional information about their work.

eMethods. Detailed Methodology

Participant recruitment.

The extended families were recruited from two sources. First, the family trees of all participants in the NIH intramural studies of ADHD were reviewed. Those with family structures meeting the inclusion criteria were contacted, had phone screening for eligibility, and if appropriate proceeded to in-person assessment at the Clinical Center of the NIH. Additionally several members of extended families contacted the study directly as a result of searching for pertinent studies into ADHD (e.g. cliniclatrials.gov). In total, 38 extended families were assessed in person at the NIH Clinical Center. Of these, 24 extended families completed the neuroimaging component of the study. All nuclear families were identified from ongoing intramural NIH studies into brain development and demographic details are given below in eTable 1. Medication histories were obtained from participants.

The diagnostic interview for adults collects information on both childhood and adult symptoms, with the help of collateral informants when available. We were thus able to determine if an adult had ADHD which persisted from childhood, showed remission or was never affected. Partial remission was defined as 3 or 4 symptoms of either hyperactivity/impulsivity or inattention that caused significant impairment in functioning at work, at home and with peers. Those with full remission had 2 or fewer symptoms in both domains with no significant impairment.

eFigure 1 and eFigure 2 show the number of individuals in each category. For adults these groups are: adult (persistent) ADHD, partial remission of ADHD; full remission of ADHD or never affected. Children were categorized as either unaffected or having ADHD. Of the children with ADHD, 23 had a combined presentation, 56 had a predominately inattentive presentation (of whom 16 had five inattentive symptoms but with clinically significant impairment that warranted diagnosis and treatment); 22 had a predominately hyperactive-impulsive presentation. Intelligence quotients

were estimated using the Wechsler Preschool and Primary Scale of Intelligence IV for participants under 6 years of age, the Wechsler Abbreviated Test of Intelligence for children between 6 and 17 years, and the Wechsler Test of Adult Reading for those 18 and over.

Neuroimaging.

Diffusion Tensor Imaging (DTI) data were acquired with a single-shot dual-spin-echo echo-planar imaging sequence with the following parameters: TE=85ms, TR=18.5s, FOV=240mm, 96x96 matrix, slice thickness = 2.5 mm, gap = 0 mm, and acceleration factor = 2. A custom set of diffusion directions and weightings were acquired for a total of 80 volumes: 10 volumes at b-value = 0 s/ mm^2, 10 volumes with evenly distributed directions at b-value=300s/ mm^2, and 60 volumes with evenly distributed directions at b-value = 1100 s/mm^2. Acquisition parameters used for children were similar, except that only 60 volumes were acquired in order to shorten the scan time: 6 volumes at b-value = 0 s/ mm^2, 12 volumes with evenly distributed directions at b-value=300s/ mm^2, and 42 volumes with evenly distributed directions at b-value = 1100 s/ mm^2. Preprocessing in the TORTOISE software package[1] included rigid body motion correction, eddy–current distortion correction, B0 distortion correction, and bicubic upsampling to 1.5mm isotropic resolution. The diffusion tensor was computed by nonlinear robust least squares fitting [2].

There were three stages of quality control. First, there was real-time re-acquisition of diffusion weighted volumes that showed motion, as judged by alignment to the first b=0s/mm2 volumes. Likely corrupted volumes were automatically pushed back to the scanner for reacquisition within the same session. Second, the final diffusion data were visually inspected and corrupted diffusion weighted volumes that had not been successfully reacquired were discarded. Individuals whose data showed >= 10% of volumes were excluded. Third, the degree of head motion was determined from the absolute value of the three translation parameters that were averaged over the registered volumes and combined using the Euclidean norm. A

similar procedure defined a rotation index for each subject. We acquired a total of 363 DTI data sets from the participants in the extended and nuclear families; 332 of these data sets passed quality control. The proportion of excluded DTI data sets did not differ by diagnosis (12/145 (8.3%) for ADHD vs 19/218 (8.7%) for unaffected ($\chi(1)2=0.02$, p=0.88).

DTI-TK software was used to register the diffusion tensors into a common template space [3,4]. It defines tracts through alignment to a template that captures the average shape and diffusion properties of tracts parcellated via modeling of sheet-like white matter fasciculi. This spatial normalization software uses the directional information of the diffusion tensors to align the data of all subjects, incorporates sequential rigid, affine, and nonlinear registration steps, and has been ranked as the top-performing tool in its class [5].

Functional connectivity was defined using a gradient-echo echo-planar series with whole-brain coverage. Parameters were: TR = 2500 ms, TE = 27 ms, flip angle = 90^{o}, 44 axial contiguous interleaved slices per volume, 2.8- mm slice thickness, FOV = 22 cm, 64 x 64 acquisition matrix. Quality control procedures are given in the main text. The EPI volumes retained after quality control were registered to the one with smallest outlier fraction, and the slice-time corrected EPI series was then co-registered to a T1-weighted anatomical image (MPRAGE). The first 3 principal components of the averaged activity in the lateral ventricles and white matter masks were used as nuisance regressors and removed using ANATICOR [6]. Those components have been shown elsewhere to be good surrogates for cardiac and respiration artifacts that often contaminate fMRI scans [7]. Finally, the time derivative of the 6 motion parameters (3 displacement, 3 rotation) were also regressed out of the activity in the TRs that had survived motion scrubbing and the subject-specific anatomical scan was non-linearly registered to a MNI template[8]. Only these residual time series were used in the rest of the analysis. A total of 340 rsFMRI data sets were acquired of which 277 passed quality control. Participants with ADHD were more likely to be excluded due to the quality control measures (31/128 (24.2%) of

ADHD compared to 32/212 (15.1%) from unaffected participants ($\chi(1)2=4.4$, $p=0.04$).

Supplemental analyses

We used SOLAR to estimate the narrow sense heritability of a trait [9,10]. This is the proportion of phenotypic variance that is attributable to additive genetic components. The heritability estimates are calculated using algorithms that employ maximum likelihood variance decomposition methods. The observed covariance matrix of the connectivity measures is contrasted against the structure of the covariance matrix predict by kinship. Connectivity measures that have larger covariance between closely related relatives than between distant relatives will have higher heritability. The significance of these heritability estimates is tested by comparing the likelihood of a model in which σ_g^2 is constrained to zero and the model in which σ_g^2 is estimated.

Where both traits were heritable, their phenotypic correlation was estimated in SOLAR, otherwise Pearson's correlations were used. In the SOLAR analyses, the phenotypic correlation between two traits (ρp) was estimated as the sum of genetic (ρg) and environmental (ρe) correlations. In brief:-

$$\rho p = \rho g\sqrt{(h^2 1 h^2 2)} + \rho e\sqrt{[(1 - h^2 1)(1 - h^2 2)]},$$

where $h^2 1$ and $h^2 2$ are the heritabilities of traits 1 and 2

If the genetic correlation coefficient (ρ_G) is significantly different from zero, then the significant portion of the variability in two traits are considered to be influenced by shared genetic factors.

Resting state network analyses.

Independent component analysis (ICA) was used to derive network maps. ICA decomposes the BOLD signal into spatially distinct maps and their time courses. Specifically, the residual time series for all subjects with clean data (i.e. extended and nuclear families) were concatenated in the time dimension to form one long

pseudo-scan with thousands of time volumes. Prior to concatenation, the data were spatially downsampled to a 5 mm grid and scaled within subject. Probabilistic ICA, as implemented in MELODIC (FMRIB, University of Oxford, UK; www.fmrib.ox.ac.uk/fsl/melodic2/index.html), was then used to extract independent components (IC). Each IC can be seen as a spatial map representing regions functionally connected in the brain (network), and these spatial maps show the strength of the contribution of every voxel in the brain to the network.
An atlas of intrinsic networks devised by Yeo and colleagues was used to categorize the different independent components into one of 7 canonical networks: visual, somatomotor, dorsal, ventral attention, affective, cognitive, and default-mode [11].
The 7 ICs (out of the 16 resulting from ICA) that showed the highest spatial correlation to the atlas were used in the analysis.

The next step used dual regression to derive the IC spatial map for each subject [12]. In short, the first step of the dual regression uses the group-level spatial maps as a set of spatial regressors in a general linear model (GLM), and thus defines the temporal dynamics associated with each group-level map. Specifically, if S is a matrix of time by voxels dimensions for a given subject, the first step of the dual regression finds matrix C (components by time), which is multiplied by the group-level matrix G (voxels by components) to result in matrix S. The second stage of the dual regression employs matrices C (result of first step), and S in another GLM to find matrix Y (components by voxels), which contains spatial maps of the representations of each IC for individual subjects. Each subject's spatial map was finally z-scored prior to heritability analyses.

Multiple comparison corrections for functional connectivity results used a non-parametric approach. Specifically, for each network we ran 500 permutations of the rsfMRI data, holding constant participant identity and family membership, but shuffling without repetition the voxel-wise data and covariates. For each permutation iteration we obtained a spatial map of voxel-wise heritability (and p-values) under the hypothesis that there was no relationship among participants'

rsfMRI data. We then determined the largest cluster seen at a voxel-wise $p < .05$ under each iteration. After running all permutations we established a null distribution of maximal cluster size. From this null distribution, we then determine the probability of seeing the observed cluster. All clusters reported were significant at a $p<0.002$.

eResults. Supplemental Findings

Heritability estimates for the white matter tract traits in extended families and association with ADHD symptoms are given in eTable 2 and eTable 3. Heritability of the intrinsic networks in the extended and nuclear families is given in eTable 4, which also details the associations with ADHD symptoms.

Association with symptom dimensions and diagnostic categories.

As detailed in the main manuscript and eTable 2, three of the 12 significantly heritable white matter tract properties were also significantly associated with symptom counts. Additionally, fractional anisotropy of the right inferior longitudinal fasciculus, which was not significantly heritable, was however associated with hyperactive-impulsive symptoms ($t=-2.32$, $p=.02$).

We analyzed data using DSM5 categories, using mixed model ANOVAs (significance set at $p<0.05$). eFigure 3 below summarizes the connectivity properties that are only associated with ADHD (using DSM-5 categories), heritable only, both heritable and ADHD-associated. For the white matter tracts, there were 15 properties that showed diagnostic group differences, of which eight were also significantly heritable.

We explored the overall group differences with post-hoc pairwise tests. There were significant pairwise differences for the right superior longitudinal fasciculus between the unaffected group and both the inattentive group (radial diffusivity $p=0.02$; axial diffusivity $p=0.01$) and combined group (radial diffusivity $p=0.02$; axial diffusivity $p=0.05$). This pattern of diagnostic group differences was in keeping with the symptoms based analyses reported in the main manuscript. There was a trend to higher radial and axial diffusivity of the left superior longitudinal fasciculus in the hyperactive-impulsive group compared to all other groups. Other diagnostic group differences emerged for fractional anisotropy. The unaffected group had higher fractional anisotropy values compared to the combined group in the right inferior

longitudinal fasciculus (p=0.02) and the left inferior fronto-occipital fasciculus (trend p=0.07). The predominately inattentive group also had higher fractional anisotropy values than the combined group in the right uncinate (p=0.002) and at a trend level for the corpus callosum (p=0.07). Finally, the never affected group had significantly higher values of radial diffusivity than the inattentive group (p=0.03) for the corpus callosum.

Resting state fMRI

In our main analyses we found that three of the four regions showing significant heritability were also associated with symptom counts. Analyzing these data using diagnostic categories we found that only the heritable region in the ventral attention network was also associated with DSM5 diagnostic categories. Here, the unaffected and inattentive groups showed significantly more connectivity within the network than the combined subtype (p=.03 and p=.01, respectively). We also investigated whether the first two principal components of the non-heritable networks were significantly associated with the DSM5 ADHD categories. No significant diagnostic associations were found.

Race/Ethnicity.

Twenty-one of the 24 extended families and 42 of the 52 nuclear families were, non-Hispanic. Three extended families and 5 nuclear families were of African American heritage. One nuclear family was of American Indian, and 4 were of Asian descent. Analyses were repeated restricting data to those who were white, non-Hispanic and the pattern of results was unchanged.

Medication analyses

Ninety-five of the 332 participants with DTI data took a psychotropic medication-details in eTable 5. Of these, 72 were taking regular psychostimulants and 35 were taking other psychotropics. For the resting state fMRI data, 79 of the 277 subjects were on a psychotropic. This included 56 who took psychostimulants and 34 on other psychotropics.

We repeated heritability analyses, removing those on psychostimulants. This did not appreciably alter heritability estimates. Specifically, only one DTI trait property (radial diffusivity of the left uncinate) lost significance. Next we removed those who were taking any psychotropic (either psychostimulant or any other psychotropic class). Again this did not have a major impact on the pattern of results. - see eTable 6.

We similarly estimated heritability within the rsfMRI data when those on psychostimulants, and then those on any psychotropic, were excluded - see eTable 7. In these analyses, we combined the extended and nuclear families and used the average of the connectivity values in each cluster as the trait, thus obtaining a single heritability estimate for the entire cluster. Connectivity within the 3 network 'hubs' was still significantly heritable even after removing participants on psychostimulants and removing those on any psychotropic.

Phenotypic correlations.

The white matter tract metrics showed high degrees of phenotypic correlation as 383 of 492 possible phenotypic trait pairs were significantly correlated (applying a FDR $q<0.05$). We illustrate one such correlation between radial diffusivity of the right inferior fronto-occipital fasciculus and axial diffusivity of the left superior longitudinal fasciculus- (significant at $p=1.E-09$, estimated in SOLAR)- eFigure 6.

Phenotypic correlations between modalities were modest but significant. eFigure 7 shows the correlation ($p=0.019$) between axial diffusivity of the right inferior fronto-occipital fasciculus and the ventral attention network (specifically the estimated connectivity of the heritable hub with the rest of the network).

Developmental analyses and results.

Trajectories of the white matter tract and resting state network metrics.

To model age related change in the connectivity measures, we compared the goodness of fit of linear mixed models which considered constant, linear and

quadratic effects of age. Family was included as a random term. The model with the lowest BIC value was chosen.

A quadratic model provided the best fit for fractional anisotropy and radial diffusivity for most tracts- parameters in eTable 8. Change in axial diffusivity was either linear or constant. eFigure 4 shows data for the right superior longitudinal fasciculus (which had quadratic fits throughout) and for the left corticospinal tract (which had a mix of quadratic and linear fits). These fits resemble prior reports of developmental change in DTI metrics [13-15]

For rsfMRI, we considered the trajectory of heritable functional connectivity within each network- shown in Figure 2. Data for the connectivity of the heritable hub within the default mode network are shown in eFigure 5. The 'y' axis shows the strength (beta coefficient) of the connectivity between the heritable 'hub' and the rest of the network. There was no age related change for the connectivity of these heritable hubs within the default mode, ventral attention and cognitive control networks (i.e. a model of constant change provided the best fit). We note that previous reports of developmental change in resting state networks have predominately used network-based statistics, which differ markedly from our dual regression based statistics [16-20].

Heritability and age.

We explored age related changes in heritability by splitting the cohort into young (<=21 years; N=150 for DTI; N=97 for rsfMRI) and adult groups (>21 years; N=149 for DTI and N=155 for rsfMRI). We calculated heritability for each age group using the same model we applied to the entire cohort. As eTable 9 shows, we found 12 tracts were significantly heritable in both the young and adult cohorts; 5 were significant in the young, and 5 in the adult cohort only.

For resting state networks, the heritability of the posterior cingulate 'hub' and the rest of the default mode network held at nominally significant levels across both the young (h^2=0.8 ± 0.24, p=0.001) and adult groups (h^2=0.38 ± 0.21, p=0.02). The

heritability of the 'hubs' was present only in the adult group for the cognitive control network (h^2=0.39 ± 0.18, p=0.01) and at a trend level for the ventral attention network (h^2=0.36 ± 0.24, p=0.06).

The impact of age on the association between symptoms and connectivity metrics. Next we determined if associations between symptoms and connectivity measures differed between the age groups. For white matter tract measures, there were no significant interactions between symptoms and the age groups that survived adjustment for multiple testing. There was a nominally significant interaction between inattentive symptoms and age group in the determination of axial diffusivity for the left IFO (β=-0.0025, t=-2.4, p=0.02). Similarly, there were nominally significant interaction between hyperactive-impulsive symptoms and age group for the fractional anisotropy of the right SLF (β=-0.003,t=-2.0, p=0.04). Thus, overall the relationships between symptoms and the white matter metrics was similar in the age groups. There were no significant interactions between symptoms and age groups in the determination of the strength of connectivity between each heritable hub and its network.

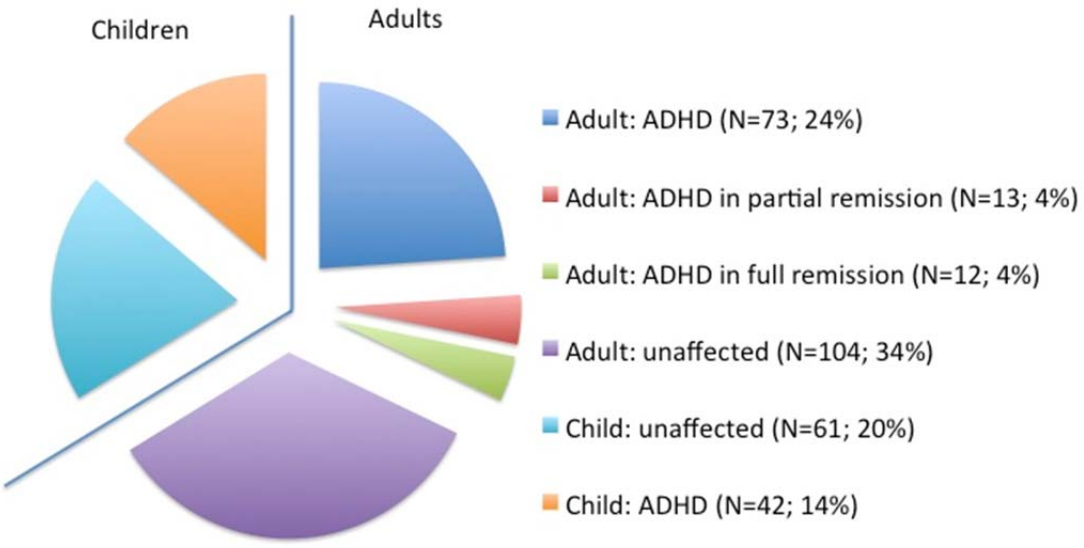

eFigure 1. Diagnostic Details for the Extended Families

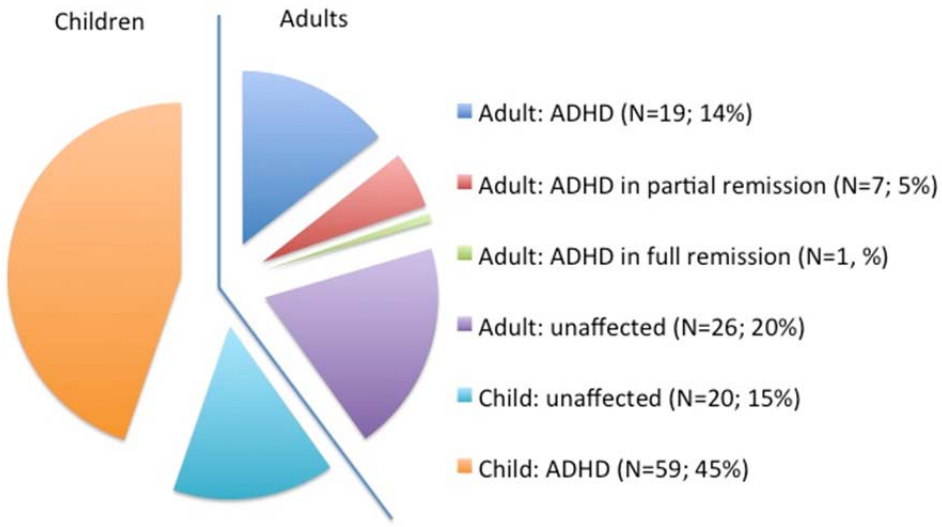

eFigure 2. Diagnostic Details for the Nuclear Families

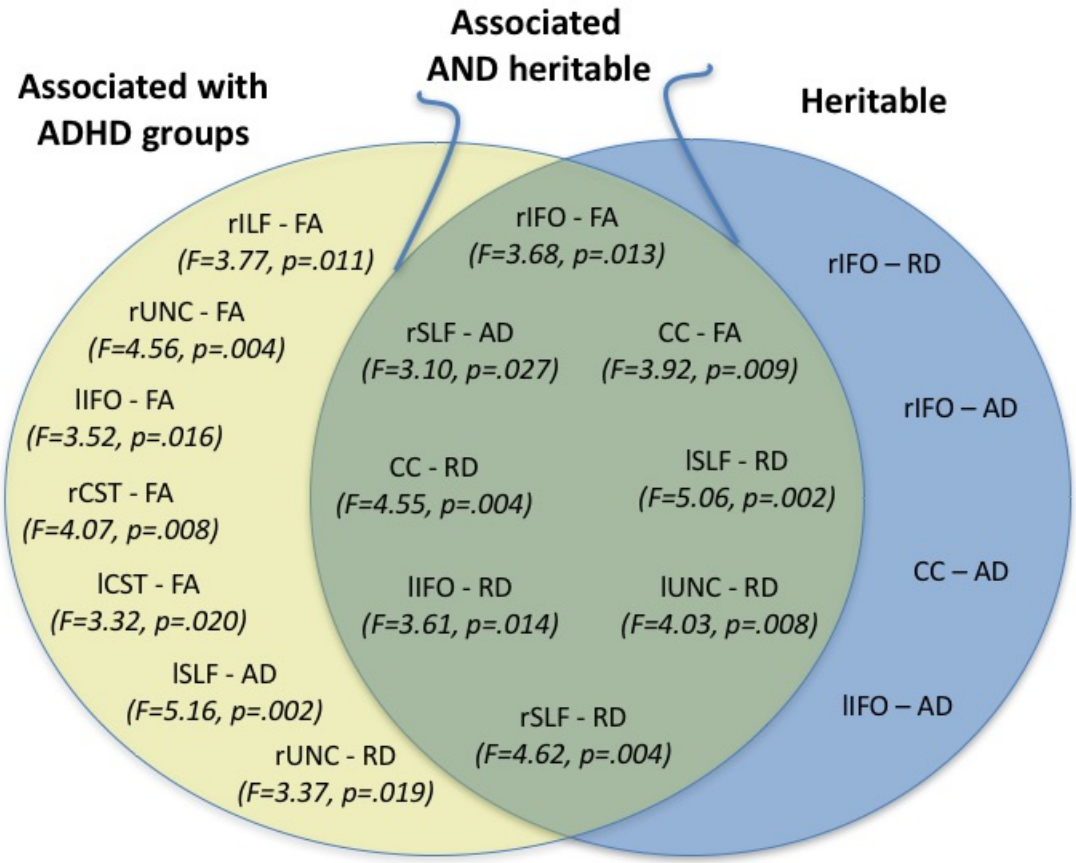

eFigure 3. White Matter Tracts Properties That Are Either Associated With ADHD Diagnostic Categories, Heritable or Both. The Venn diagram shows tract properties that only associated with ADHD groups (in yellow) or both associated with ADHD groups and heritable (green). Tract properties that are only heritable (and did not show diagnostic group differences) are in blue. The F value is given for the group differences (between combined, inattentive, hyperactive-impulsive and unaffected) where significant at $p<0.05$. Abbreviations: SLF = superior longitudinal fasciculus; ILF = inferior longitudinal fasciculus; UNC = uncinate; IFO = inferior fronto-occipital fasciculus; CC = corpus callosum; l=left; r=right.

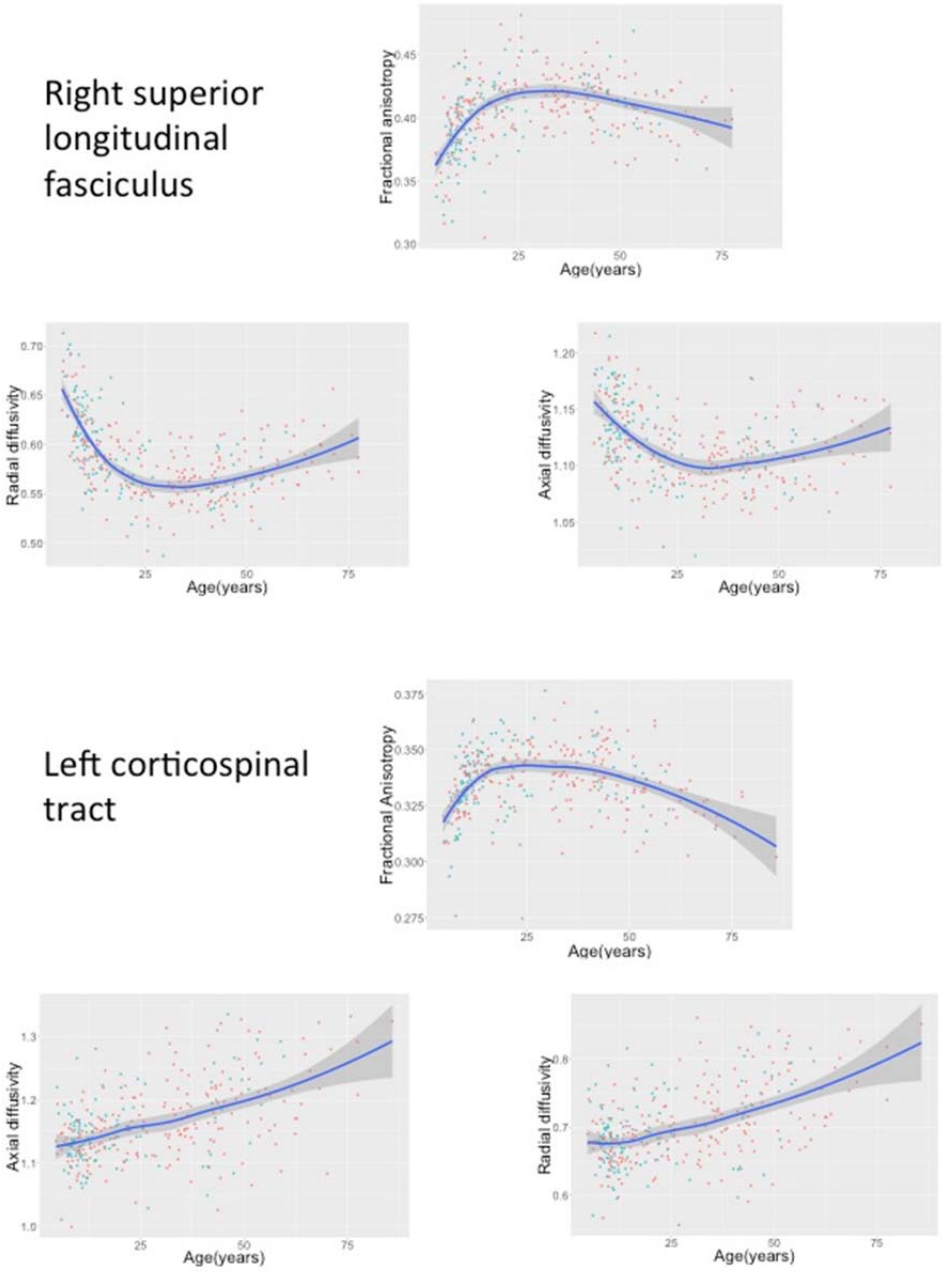

eFigure 4. Diffusion Values Are Given for the Right Superior Longitudinal Fasciculus and for the Left Corticospinal Tract. Data for extended families are given in orange and for nuclear families in blue and locally weighted smoothing (LOESS) line is superimposed.

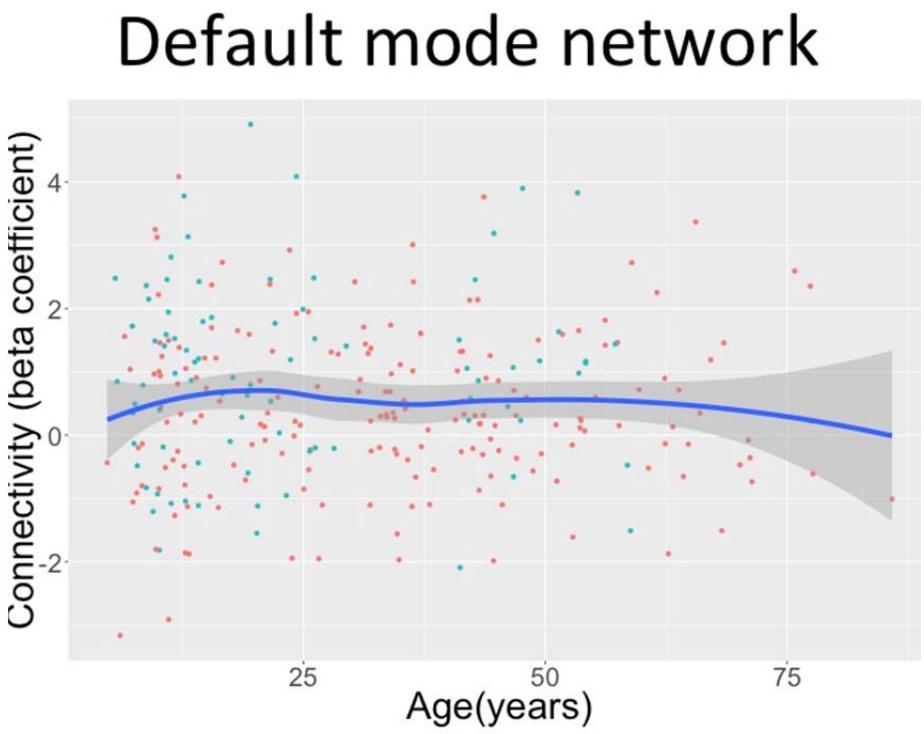

eFigure 5. The Functional Connectivity of the Posterior Cingulate Hub With the Remainder of the DMN. A locally weighted smoothing line is superimposed. There was no age related change in the connectivity measure.

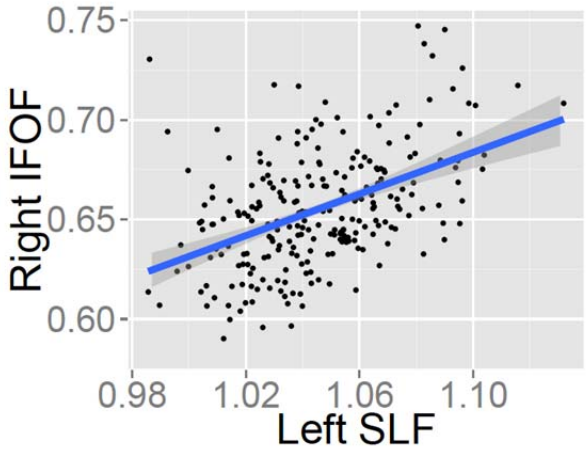

eFigure 6. Correlation Between Radial Diffusivity of the Right Inferior Fronto-Occipital Fasciculus and Axial Diffusivity of the Left Superior Longitudinal.

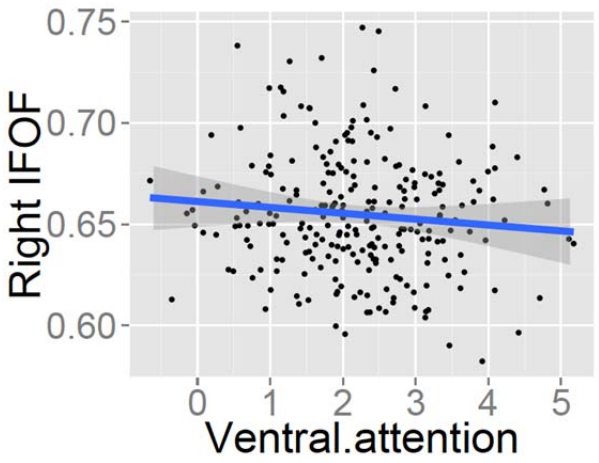

eFigure 7. Correlation Between Radial Diffusivity of the Right Inferior Fronto-Occipital Fasciculus and the Connectivity of the Heritable Hub Within the Ventral Attention Network.

eTable 1. Demographic Details of Nuclear Families With Clinical and Imaging Phenotypes.

	Nuclear families	Individuals within nuclear families
Clinical phenotypes available (N)	52	132
Affected: N (%)	-	78 (59%)
Age (years) – mean (SD)	-	20.9(15)
Age (years) - range	-	4 to 49
Sex: male (%)/female (%)	-	86 (65%)/ 46 (35%)
Brain phenotypes		
White matter tracts (DTI)	47	119
Resting state networks (rsFMRI)	33	84

eTable 2. Heritability of White Matter Tracts. Significant values for extended families (surviving Bonferroni adjustment) are in bold. RD=radial diffusivity, FA= fractional anisotropy, AD= axial diffusivity

Fasciculus (white matter tract)	Extended families	Nuclear families	
	h2 (SE), p value	Con-firmed	h2 (SE), p value
R superior longitudinal -RD	**0.69 (0.13), p= 0.0000002**	YES	0.46 (0.16), p=0.002
R superior longitudinal -AD	**0.60 (0.15), p= 0.00003**	YES	0.43 (0.23), p=0.03
R inferior fronto-occipital -FA	**0.46 (0.15), p= 0.0009**	YES	0.95 (0.08), p=0.000003
R inferior fronto-occipital -RD	**0.67 (0.14), p= 0.0000005**	YES	0.50 (0.23), p=0.01
L inferior fronto-occipital -RD	**0.66 (0.13), p= 0.0000004**	YES	0.84 (0.11), p=0.000004
L inferior fronto-occipital -AD	**0.50 (0.16), p= 0.0004**	YES	0.63 (0.24), p=0.002
R inferior fronto-occipital -AD	**0.45 (0.15), p= 0.0005**	YES	0.35 (0.2), p=0.03
Corpus callosum -RD	**0.56 (0.13), p= 0.000001**	YES	0.62 (0.13), p=0.00008
Corpus callosum -FA	**0.54 (0.14), p= 0.00004**	YES	0.65 (0.13), p=0.00002
Corpus callosum -AD	**0.44 (0.14), p= 0.0003**	YES	0.67 (0.14), p=0.0001
L uncinate -RD	**0.5 (0.16), p= 0.0004**	YES	0.60 (0.23), p=0.005
L superior longitudinal -RD	**0.51 (0.12), p= 0.00002**	YES	0.42 (0.16), p=0.005
L superior longitudinal -AD	**0.49 (0.14), p= 0.0001**	NO	0.2 (0.24), p=0.2
R superior longitudinal -FA	**0.46 (0.14), p= 0.0003**	NO	0 (0), p=0.5
R uncinate -FA	0.39 (0.14), p= 0.002		
L uncinate -FA	0.38 (0.15), p= 0.005		
R inferior longitudinal -RD	0.38 (0.15), p= 0.003		
L uncinate -AD	0.36 (0.16), p= 0.005		
L superior longitudinal -FA	0.32 (0.13), p= 0.004		
L corticospinal -RD	0.32 (0.16), p= 0.01		
L inferior fronto-occipital -FA	0.3 (0.15), p= 0.02		
R corticospinal -AD	0.29 (0.13), p= 0.006		
L corticospinal -FA	0.28 (0.13), p= 0.01		
R corticospinal -RD	0.26 (0.14), p= 0.02		
R corticospinal -FA	0.25 (0.14), p= 0.03		
L corticospinal -AD	0.2 (0.14), p= 0.05		
L inferior longitudinal -RD	0.2 (0.12), p= 0.04		
L inferior longitudinal -AD	0.19 (0.16), p= 0.09		
R uncinate -RD	0.18 (0.15), p= 0.1		
R uncinate -AD	0.12 (0.15), p= 0.21		
R inferior longitudinal -FA	0 (0), p= 0.5		
L inferior longitudinal -FA	0 (0), p= 0.5		
R inferior longitudinal -AD	0 (0), p= 0.5		

eTable 3. White Matter Tract Heritability for the Entire Cohort and Association With ADHD Symptoms. Significant associations are in bold. *= survives Bonferroni adjustment.

Fasciculus	Entire cohort	Association with ADHD	
	h2 (SE), p value	Inattention: t (p)	Hyperactivity-impulsivity: t (p)
R superior longitudinal -RD	**0.61 (0.1), p=0.000000002**	**t=-3.05 (p=0.003)***	t=-0.26 ,ns
R superior longitudinal -AD	**0.48 (0.13), p=0.00003**	**t=-2.51 (p=0.01)**	t=-1.11 ,ns
R inferior fronto-occipital -FA	**0.59 (0.12), p=0.0000004**	t=-0.58 ,ns	**t=-2.35 (p=0.02)**
R inferior fronto-occipital -RD	0.57 (0.12), p=0.0000001	t=-0.74 ,ns	t=1.17 ,ns
L inferior fronto-occipital -RD	0.69 (0.1), p=0.0000000003	t=0.18 ,ns	t=1.05 ,ns
L inferior fronto-occipital -AD	0.52 (0.13), p=0.000005	t=-0.01 ,ns	t=0.27 ,ns
R inferior fronto-occipital -AD	0.37 (0.12), p=0.0003	t=-1.84 ,ns	t=-0.96 ,ns
Corpus callosum –RD	0.53 (0.1), p=0.00000005	t=-1.79 ,ns	t=0.61 ,ns
Corpus callosum –FA	0.58 (0.1), p=0.000000009	t=1.06 ,ns	t=-1.24 ,ns
Corpus callosum –AD	0.48 (0.11), p=0.000005	t=-1.25 ,ns	t=0.66 ,ns
L uncinate –RD	0.44 (0.13), p=0.0001	t=0.8 ,ns	t=0.87 ,ns
L superior longitudinal -RD	0.47 (0.1), p=0.0000009	t=-1.08 ,ns	t=1.06 ,ns

eTable 4. Heritability of the Intrinsic Functional Networks in Extended and Nuclear Families and Association With ADHD.

	Extended families			Nuclear families		Association with ADHD symptoms
Network	Region (MNI coords)	H^2 (SE)	Cluster (mm^3)	Confirmed	H^2 (SE)	
Default mode	L posterior cingulate (-6,-59,11)	.36 (.16)	5125	Yes	.61 (.24)	Inattention (t=-2.34, p=0.02) Hyperactive-impulsive (t=-2.63, p=.008)
Ventral attention	R superior frontal gyrus (25, 53, 19)	.36 (.16)	4500	Yes	.58 (.24)	Hyperactive-impulsive (t=-2.76, p=0.006)
Cognitive control	R supramarginal gyrus (52,-41,38)	.32 (.15)	6500	Yes	.46 (.25)	N.S.

eTable 5. The Number of Participants on Psychostimulant and Other Psychotropic Medications. Note that as one person can take more than one medication the total taking any psychotropic is lower than the sum of the individual medications.

	White matter tracts (DTI)	Resting state fMRI
Any psychotropic	95	79
Psychostimulants		
-Methylphenidate based	34	26
-Amphetamine based	38	30
Other psychotropics		
Any psychotropic	35	34
-SSRI	22	19
-Buproprion	8	9
-Guanfacine	2	1
-Atomoxetine	2	2
-Mood stabilizers	2	2
-Benzodiazepines	1	3

eTable 6. Heritability of the White Matter Tracts Excluding Those on Psychostimulants and Those on Any Psychotropics. Only previously confirmed results are shown. Results surviving Bonferroni correction (over all traits) are in bold.

Fasciculus (white matter tract)	No psychostimulants (N=260) h2 (SE), p value	No psychotropics (N=237) h2 (SE), p value
R superior longitudinal -RD	**0.76 (0.11), p=5.4*10^{-10}**	**0.75 (0.11), p=4.7*10^{-10}**
R superior longitudinal -AD	**0.58 (0.13), p= 0.00003**	**0.58 (0.14), p=0.0001**
R inferior fronto-occipital -FA	**0.62 (0.13), p= 0.000006**	**0.63 (0.13), p=0.000005**
R inferior fronto-occipital -RD	**0.70 (0.14), p= 0.0000004**	**0.71 (0.14), p=0.0000007**
L inferior fronto-occipital -RD	**0.76 (0.10), p= 1.2*10^{-9}**	**0.68 (0.12), p=0.0000003**
L inferior fronto-occipital -AD	**0.56 (0.15), p= 0.00005**	**0.56 (0.16), p=0.0001**
R inferior fronto-occipital -AD	**0.50 (0.16), p= 0.0003**	**0.52 (0.17), p=0.0005**
Corpus callosum –RD	**0.53 (0.11), p= 0.000005**	**0.52 (0.12), p=0.00001**
Corpus callosum –FA	**0.56 (0.12), p= 0.000006**	**0.50 (0.13), p=0.00006**
Corpus callosum –AD	**0.53 (0.13), p= 0.00007**	**0.51 (0.14), p=0.0002**
L uncinate –RD	0.46 (0.16), p= 0.001	0.39 (0.16), p=0.005
L superior longitudinal -RD	**0.65 (0.11), p= 0.0000001**	**0.68 (0.12), p=0.0000001**

eTable 7. Heritability of Functional Connectivity Within Intrinsic Networks, Excluding Those on Psychostimulants and Those on Any Psychotropics.

	Entire cohort (N=277)		No psychostimulants (N=221)	No psychotropics (N=198)
Network	Region (MNI coordinates)	h2 (SE), p value	h2 (SE), p value	h2 (SE), p value
Default mode	L posterior cingulate (-6,-59,11)	0.65 (0.12), p= 0.0000001	0.74 (0.13), p= 0.0000008	0.77 (0.13), p= 0.000001
Ventral attention	R superior frontal gyrus (25, 53, 19)	0.53 (0.13), p= 0.00004	0.63 (0.15), p= 0.00004	0.61 (0.15), p= 0.0001
Cognitive control	R supramarginal gyrus (52,-41,38)	0.46 (0.12), p= 0.00004	0.37 (0.14), p= 0.003	0.42 (0.15), p= 0.002

eTable 8. The Best Fitting Age Model for Each Tract Property Is Given. Code: CC=corpus callosum; CST=corticospinal tract; IFOF=inferior fronto-occipital fasciculus; ILF=inferior frontal fasciculus; UNC=uncinate.

Tract	DTI	Fit (BIC)	Linear age (beta)	SE	P value	Quadratic age (beta)	SE	P value
CC	FA	Quadratic	1.87E-03	1.41E-04	6.88E-31	-2.68E-05	1.95E-06	1.49E-32
CC	RD	Quadratic	-2.11E-03	3.35E-04	1.26E-09	3.74E-05	4.66E-06	4.16E-14
L CST	FA	Quadratic	1.22E-03	1.49E-04	1.39E-14	-1.77E-05	2.09E-06	1.85E-15
L IFOF	FA	Quadratic	2.68E-03	1.92E-04	2.46E-33	-3.50E-05	2.68E-06	2.34E-30
L IFOF	RD	Quadratic	-4.08E-03	2.91E-04	1.32E-33	5.35E-05	4.07E-06	1.50E-30
L ILF	RD	Quadratic	-3.44E-03	4.26E-04	2.72E-14	4.32E-05	5.95E-06	4.83E-12
L SLF	AD	Quadratic	-2.87E-03	2.87E-04	4.32E-20	3.52E-05	4.10E-06	9.15E-16
L SLF	FA	Quadratic	2.32E-03	1.87E-04	4.64E-28	-3.01E-05	2.60E-06	2.80E-25
L SLF	RD	Quadratic	-4.22E-03	3.06E-04	7.47E-33	5.35E-05	4.31E-06	5.37E-28
L UNC	FA	Quadratic	2.18E-03	2.08E-04	1.31E-21	-2.57E-05	2.92E-06	2.01E-16
L UNC	RD	Quadratic	-3.43E-03	3.31E-04	3.51E-21	4.11E-05	4.66E-06	1.73E-16
R CST	FA	Quadratic	1.37E-03	1.46E-04	3.85E-18	-1.92E-05	2.06E-06	5.09E-18
R IFOF	FA	Quadratic	2.51E-03	1.99E-04	1.16E-28	-3.47E-05	2.77E-06	2.12E-28
R IFOF	RD	Quadratic	-3.08E-03	3.24E-04	1.78E-18	4.46E-05	4.67E-06	1.09E-18
R ILF	FA	Quadratic	2.11E-03	2.96E-04	1.08E-11	-2.51E-05	4.16E-06	5.42E-09
R ILF	RD	Quadratic	-4.07E-03	3.93E-04	2.84E-21	5.00E-05	5.61E-06	9.97E-17
R SLF	AD	Quadratic	-3.11E-03	3.40E-04	1.86E-17	3.79E-05	4.84E-06	1.40E-13
R SLF	FA	Quadratic	2.76E-03	2.70E-04	6.78E-21	-3.50E-05	3.82E-06	1.91E-17
R SLF	RD	Quadratic	-4.78E-03	3.38E-04	6.24E-34	5.92E-05	4.79E-06	6.96E-28
R UNC	FA	Quadratic	2.23E-03	2.11E-04	7.80E-22	-2.61E-05	2.96E-06	1.77E-16
R UNC	RD	Quadratic	-4.43E-03	3.89E-04	1.39E-24	5.44E-05	5.48E-06	7.59E-20
L CST	AD	Linear	1.70E-03	1.66E-04	1.18E-20			
L CST	RD	Linear	1.53E-03	1.55E-04	1.28E-19			
R CST	AD	Linear	1.41E-03	1.55E-04	3.00E-17			
R CST	RD	Linear	1.28E-03	1.40E-04	1.84E-17			
CC	AD	constant	-					
L IFOF	AD	constant	-					
L ILF	AD	constant	-					
L ILF	FA	constant	-					
L UNC	AD	constant	-					
R IFOF	AD	constant	-					
R ILF	AD	constant	-					
R UNC	AD	constant	-					

eTable 9. Heritability of White Matter Tract Metrics in Young (21 and Under) and Adult Age Groups. *= nominally significant at p<0.05; ** indicates significant following Bonferroni correction. N/A= not estimated.

Tract	Property	h^{2-} youth	P value	h^{2-} adult	P value
L IFOF	FA	0.74 (0.19)	0.0002**	0.65 (0.2)	0.0009**
CC	FA	0.65 (0.15)	0.0001**	0.6 (0.2)	0.001**
R SLF	RD	0.96 (0.06)	0.000002**	0.59 (0.21)	0.002*
L SLF	RD	0.96 (0.04)	0.0000001**	0.57 (0.21)	0.005*
R IFOF	FA	0.96 (0.06)	0.0000002**	0.46 (0.21)	0.02*
L UNC	RD	0.65 (0.17)	0.0005**	0.38 (0.23)	0.04*
L IFOF	RD	0.49 (022)	0.02*	0.8 (0.18)	0.00007**
CC	RD	0.49 (0.16)	0.004*	0.73 (0.21)	0.0001**
CC	AD	0.48 (0.18)	0.006*	0.52 (0.22)	0.006*
R IFOF	RD	0.62 (0.21)	0.002*	0.45 (0.21)	0.01*
L ILF	RD	0.36 (0.17)	0.03*	0.27 (0.18)	0.05*
R CST	FA	0.52 (0.17)	0.003*	0.33 (0.2)	0.05*
L UNC	FA	0.78 (0.16)	0.00004**	0.41 (0.29)	0.08
L CST	FA	0.60 (0.18)	0.0005**	0.3 (0.22)	0.08
R ILF	RD	0.58 (0.13)	0.0004**	0.2 (0.18)	0.12
R UNC	FA	0.86 (0.09)	0.000001**	0.23 (0.24)	0.16
R IFOF	AD	0.5 (0.21)	0.01*	0.23 (0.24)	0.15
R SLF	AD	0.33 (0.22)	0.06	0.71 (0.23)	0.001*
R CST	AD	0.003 (0.22)	0.49	0.36 (0.18)	0.01*
R SLF	FA	N/A		0.38 (0.2)	0.02*
L IFOF	AD	0.25 (0.23)	0.14	0.43 (0.24)	0.03*
L CST	AD	0.04 (0.2)	0.42	0.34 (0.22)	0.05*
L ILF	AD	0.265 (0.22)	0.13	0.01 (0.23)	0.48
L SLF	AD	0.32 (0.24)	0.09	0.34 (0.24)	0.07
L UNC	AD	0.31 (0.23)	0.08	0.16 (0.18)	0.18
R ILF	AD	0.1 (0.21)	0.31	0.02 (0.18)	0.46
R UNC	AD	0.07 (0.22)	0.37	0.02 (0.19)	0.46
L ILF	FA	0.13 (0.19)	0.25	N/A	
L SLF	FA	N/A		0.29 (0.2)	0.07
R ILF	FA	0.23 (0.21)	0.13	0.04 (0.2)	0.41
L CST	RD	0.09 (0.22)	0.34	0.24 (0.23)	0.13
R CST	RD	0.22 (0.24)	0.17	0.32 (0.22)	0.06
R UNC	RD	0.19 (0.2)	0.17	N/A	

eReferences.

1. Pierpaoli C, Walker L, Irfanoglu M, et al. TORTOISE: an integrated software package for processing of diffusion MRI data. *Book TORTOISE: an integrated software package for processing of diffusion MRI data (Editor ed.^ eds.).* 2010;18:1597.
2. Basser PJ, Pierpaoli C. Microstructural and physiological features of tissues elucidated by quantitative-diffusion-tensor MRI. *Journal of Magnetic Resonance, Series B.* 1996;111(3):209-219.
3. Zhang H, Avants BB, Yushkevich PA, et al. High-Dimensional Spatial Normalization of Diffusion Tensor Images Improves the Detection of White Matter Differences: An Example Study Using Amyotrophic Lateral Sclerosis. *Medical Imaging, IEEE Transactions on.* 2007;26(11):1585-1597.
4. Zhang H, Yushkevich P, Rueckert D, Gee J. A computational DTI template for aging studies. Paper presented at: Proc ISMRM2009.
5. Wang Y, Gupta A, Liu Z, et al. DTI registration in atlas based fiber analysis of infantile Krabbe disease. *Neuroimage.* 2011;55(4):1577-1586.
6. Jo HJ, Saad ZS, Simmons WK, Milbury LA, Cox RW. Mapping sources of correlation in resting state FMRI, with artifact detection and removal. *Neuroimage.* 2010;52(2):571-582.
7. Behzadi Y, Restom K, Liau J, Liu TT. A component based noise correction method (CompCor) for BOLD and perfusion based fMRI. *Neuroimage.* 2007;37(1):90-101.
8. Holmes CJ, Hoge R, Collins L, Woods R, Toga AW, Evans AC. Enhancement of MR images using registration for signal averaging. *J Comput Assist Tomogr.* 1998;22(2):324-333.
9. Blangero J, Almasy L. Solar: sequential oligogenic linkage analysis routines. *Population Genetics Laboratory Technical Report.* 1996;6.
10. Almasy L, Blangero J. Multipoint Quantitative-Trait Linkage Analysis in General Pedigrees. *The American Journal of Human Genetics.* 1998;62(5):1198-1211.
11. Yeo BT, Krienen FM, Sepulcre J, et al. The organization of the human cerebral cortex estimated by intrinsic functional connectivity. *Journal of neurophysiology.* 2011;106(3):1125-1165.
12. Beckmann CF, Mackay CE, Filippini N, Smith SM. Group comparison of resting-state FMRI data using multi-subject ICA and dual regression. *Neuroimage.* 2009;47(Suppl 1):S148.
13. Lebel C, Gee M, Camicioli R, Wieler M, Martin W, Beaulieu C. Diffusion tensor imaging of white matter tract evolution over the lifespan. *Neuroimage.* 2012;60(1):340-352.
14. Lebel C, Beaulieu C. Longitudinal development of human brain wiring continues from childhood into adulthood. *The Journal of Neuroscience.* 2011;31(30):10937-10947.

15. Simmonds DJ, Hallquist MN, Asato M, Luna B. Developmental stages and sex differences of white matter and behavioral development through adolescence: a longitudinal diffusion tensor imaging (DTI) study. *Neuroimage.* 2014;92:356-368.
16. Uddin LQ, Supekar K, Menon V. Typical and atypical development of functional human brain networks: insights from resting-state fMRI. *Frontiers in Systems Neuroscience.* 2010;4.
17. Dosenbach NUF, Nardos B, Cohen AL, et al. Prediction of Individual Brain Maturity Using fMRI. *Science.* 2010;329(5997):1358-1361.
18. Tomasi D, Volkow ND. Aging and functional brain networks. *Molecular psychiatry.* 2012;17(5):549-558.
19. Wu K, Taki Y, Sato K, et al. Topological organization of functional brain networks in healthy children: differences in relation to age, sex, and intelligence. *PloS one.* 2013;8(2):e55347.
20. Zuo X-N, Kelly C, Di Martino A, et al. Growing together and growing apart: regional and sex differences in the lifespan developmental trajectories of functional homotopy. *The Journal of neuroscience.* 2010;30(45):15034-15043.

